34th Annual International Conference of the IEEE EMBS
San Diego, California USA, 28 August - 1 September, 2012

An adaptive weighting approach for ensemble-based detection of microaneurysms in color fundus images

Bálint Antal, István Lázár and András Hajdu

Abstract— **In this paper, we present an adaptive weighting approach to microaneurysm detector ensembles. The basis of the adaptive weighting approach is the spatial location and contrast of the detected microaneurysm. During training, the performance of ensemble members is measured with a respect to these contextual information, which serves as a basis for the optimal weights assigned to detectors. We have tested this approach on two publicly available datasets, where it showed its competitiveness compared with out previously published ensemble-based approach for microaneurysm detection. Moreover, the proposed approach outperformed all the investigated individual detectors.**

I. Introduction

Diabetic retinopathy (DR) is a serious eye disease that originates from diabetes mellitus and is the most common cause of blindness in the developed countries. Early treatment can prevent patients to become affected from this condition or at least the progression of DR can be slowed down. One of the earliest signs of DR are microaneurysms (MAs). Thus it is essential to recognize this lesion in the fundus of the eye in time. Computer-aided MA detection is based on the detailed analysis of digital fundus images (see Figure 1 for an example). MAs appear as small circular dark spots on the surface of the retina.

In [1], we introduced ⟨preprocessing method, candidate extractor⟩ ensembles for MA detection, which are effective tools for increasing the sensitivity of microaneurysm detectors by fusing the detections of the candidate extractors applied after different preprocessing methods. In [2], we introduced a selection technique for ⟨preprocessing method, candidate extractor⟩ ensembles, which resulted in the first ranked microaneurysm detector in the Reintopathy Online Challenge [3].

In this paper, we present an adaptive weighting approach for ⟨preprocessing method, candidate extractor⟩ ensembles. This approach assigns an optimal weight for each member of the ensemble based on their performance of detecting MAs having different contrast and spatial locations. The experimental results show that this method is competitive with our former ensemble-selection approach [2].

This work is supported by the TAMOP-4.2.2/B-10/1-2010-0024 project, which is co-financed by the EU and the European Social Fund. This work is also supported by the OTKA (project number NK101680) and by the TECH08-2 project DRSCREEN - Developing a computer based image processing system for diabetic retinopathy screening (contract no.: OM-00194/2008, OM-00195/2008, OM-00196/2008).We are also thankful for the organizers of the Retinopathy Online Challenge for their help.

B. Antal, I. Lázár and A. Hajdu are with Faculty of Informatics, University of Debrecen, 4010 Debrecen, POB 12, Hungary. E-mail: {*antal.balint, lazar.istvan, hajdu.andras*}*@inf.unideb.hu*

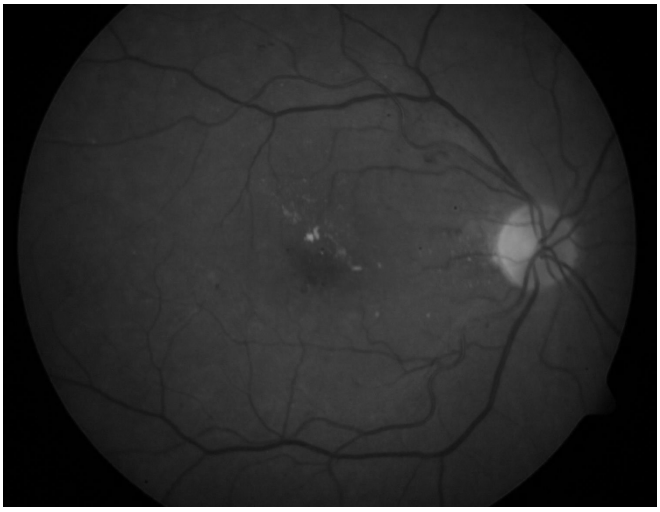

Fig. 1. An example fundus image from the DiaretDB0 [4] dataset.

The rest of the paper is organized as follows: in section II, we briefly describe the preprocessing methods involved in our study, while the MA candidate extractors are presented in section III. The concept of ⟨preprocessing method, candidate extractor⟩ ensembles is described in section IV, as well as the proposed adaptive weighting approach. Section V is devoted to the methodology we used in this paper. In section VI, we discuss our experimental results, while we draw conclusions in section VII.

II. Preprocessing methods

In this section, we present the preprocessing methods which we apply on color fundus images to correct the imaging errors they suffer from. The selection of these methods reflects the literature recommendations mentioned in the introduction.

A. Walter-Klein contrast enhancement [5]

This preprocessing method stretches the contrast of fundus images with the following gray level transformation:

$$f' = \begin{cases} \dfrac{\frac{1}{2}\left(f'_{max} - f'_{min}\right)}{\left(\mu - f_{min}\right)^r}\left(f - f_{min}\right)^r + f'_{min}, & f \le \mu, \\ \dfrac{-\frac{1}{2}\left(f'_{max} - f'_{min}\right)}{\left(\mu - f_{max}\right)^r}\left(f - f_{max}\right)^r + f'_{max}, & f \ge \mu, \end{cases} \tag{1}$$

where $\{f_{min}, \ldots, f_{max}\}$, $\{f'_{min}, \ldots, f'_{max}\}$ are the intensity levels of the original and the enhanced image, respec-

tively, μ is the mean value of the original grayscale image and $r \in \mathbb{R}$ is a transition parameter.

B. Contrast Limited Adaptive Histogram Equalization [6]

First, an adaptive histogram equalization is applied, where the intensities having a larger frequencies than a predefined threshold are clipped. Finally, a bilinear interpolation is applied to eliminate the boundaries between the regions.

C. Gray-World Normalization [7]

Each pixel on the green channel of the image is transformed in the following way:

$$f' = \frac{f}{\mu}, \tag{2}$$

where f' and f are the respective new and the original pixel intensities and μ is the average intensity of the green channel.

D. Intensity adjustment [8]

This preprocessing method enhances the contrast of a grayscale image by saturating the lowest and highest 1% of the intensity values.

E. Illumination Equalization [9]

This preprocessing method tackles the problems caused by the uneven illumination of retinal images. Each pixel intensity is set according to the following formula:

$$f' = f + \mu_d - \mu_l, \tag{3}$$

where f, f' are the respective original and the new pixel intensity values, μ_d is the desired average intensity and μ_l is the local average intensity.

F. Vessel Removal and Interpolation [10]

The complete vessel system is removed and the holes are filled by inpainting [11].

G. Wiener filter [12]

This filter passes low frequency components based on statistics estimated from a local neighbourhood of each pixel.

H. No preprocessing

We also consider the results of the candidate extractors obtained for the original images without any preprocessing.

III. MA candidate extraction

Candidate extraction is a process which aims to spot objects in the image showing MA-like characteristics. Individual MA detectors follow their own way to extract MA candidates. In this section, we provide a brief overview of the candidate extractors involved in our analysis. These algorithms realize different approaches that were described in details in the introduction.

A. Walter et al. [13]

Candidate extraction is accomplished by grayscale diameter closing, which aims to find all sufficiently small dark patterns on the green channel. After that, a double thresholding is applied.

B. Spencer et al. [14]

The vascular map is extracted by applying twelve morphological top-hat transformations with twelve rotated linear structuring elements (with a radial resolution $15\,^\circ$). Then, the vascular map is subtracted from the input image, which is followed by the application of a Gaussian matched filter. The resulting image is then binarized with a fixed threshold and the shapes of the MAs are approximated by region growing.

C. Circular Hough-transformation [15]

Following the idea presented in [15], we established an approach based on the detection of small circular spots in the image. Candidates are obtained by detecting circles on the images using circular Hough transformation [16]. With this technique, a set of approximately circle-shaped objects can be extracted from the image.

D. Zhang et al. [17]

In order to extract candidates, this method considers the maximal correlation coefficient with five Gaussian masks with different standard deviations for each pixel. Then, it is thresholded with a fixed threshold value to obtain the candidates.

E. Lazar et al. [18]

This approach starts with a pixel-wise cross-section profile alignment with multiple orientations. Then, multi-directional height map is constructed, which assigns a set of values to each pixel. These values describe the distinction of the pixel from its surrounding in a particular direction. After that, MAs are extracted by thresholding of score values computed from the directional height map.

IV. The adaptive weighting approach for ⟨preprocessing method, candidate extractor⟩ ensembles

A ⟨preprocessing method, candidate extractor⟩ ensemble is a set $S = \{\langle PP_i, CE_j\rangle | i = 1, \ldots, M, j = 1, \ldots, N\}$ containing all ⟨preprocessing method, candidate extractor⟩ pairs, where M is the number of preprocessing methods and N is the number of candidate extractors, respectively. In this way, a pair from each preprocessing method and candidate extractor is formed by generating the output of the candidate extractor on the training images with the given preprocessing method applied.

In this paper, we combine the outputs of the ⟨preprocessing method, candidate extractor⟩ pairs by weighting. We assign weights for each candidate with a respect to three different kind of information: which pair detected the candidate, what is the contrast in the neighbourhood of the MA and where it is located on the image.

A. Categorization of MAs based on visibility

To measure the visibility of an MA, we select an e. g. $K \times L = 20 \times 20$ window centered on the MA centroid and

measure the contrast in this region in the following way:

$$\sqrt{\frac{1}{MN}\sum_{x=1}^{M}\sum_{y=1}^{N}\left(I_{xy}-\mu\right)^2}, \tag{4}$$

where I_{xy} is the corresponding intensity of the pixel having coordinates (x, y) and μ is the average intensity of the window. The optimal number of K and L can be determined experimentally.

Since we do not have any prior knowledge about the distribution of MAs based on the contrast information, we aimed to divide the MAs into three sets with equal cardinalities. Thus, we categorize an MA as *subtle*, if its contrast is lower than the 33th percentile of the observed contrast values in the training set, *obvious*, if its contrast is higher than the 66th percentile and *regular*, otherwise.

B. Categorization of MAs based on spatial location

We also categorized MAs into four more categories based on their spatial location: *near to vessel*, *in the macula*, *on the periphery* or *other*. For the first category, we must detect the vessel system of the retina. For this task, we used the method presented in [19]. We consider an MA as *near to vessel*, if it is closer to a vessel part than the maximal MA diameter. For the second category, we detected the macula with the method proposed in [20]. Then, we classify the MAs falling into the area of the macula belonging to the *in the macula* category. Finally, MAs *on the periphery* are determined in the following way: first, the radius of the retinal ROI is calculated (based on the ROI detection result using the algorithm proposed in [21]), then, each MAs having the distance at least the e. g. 90% of the radius from the center of the retina is considered as peripheral MA. The aforementioned distance can be adjusted basedon experiments. MAs do not fit in the above described three spatial categories are considered in the *other* category.

C. Weighting

The performance of each ⟨preprocessing method, candidate extractor⟩ pair is measured for each category in the following way: each extracted candidate is categorized both by visibility and spatial location, then compared to the ground truth whether it is an actual MA or not. Based on this evaluation, for each pair p, visual category v and spatial category s, we calculate the F-score [22] measure:

$$f_{vs}^{p}=\frac{2\cdot sen_{vs}^{p}\cdot ppv_{vs}^{p}}{sen_{vs}^{p}+ppv_{vs}^{p}}, \tag{5}$$

where

$$sen=\frac{\text{True MA candidates}}{\text{All MAs}}, \tag{6}$$

$$ppv=\frac{\text{True MA candidates}}{\text{All MA candidates}}, \tag{7}$$

$$v\in\{\text{subtle},\text{obvious},\text{regular}\}, \tag{8}$$

and

$$s\in\{\text{near to vessel},\text{in the macula},\text{on the periphery},\text{other}\}.$$

Then, we approximate the optimal weights for ⟨preprocessing method, candidate extractor⟩ pair p through the following formula [23]:

$$w_{vs}^{p}=\log\frac{f_{vs}^{p}}{1-f_{vs}^{p}}. \tag{9}$$

The weights are normalized for each combination of visual and spatial categories to have a sum of 1.

Finally, for each candidate on an unknown image, the visual and spatial location categories are determined and the corresponding weight values are summed as to the confidence value of the MA candidate. The final confidence value assigned to an MA candidate is the sum of the weights of the ⟨preprocessing method, candidate extractor⟩ pairs, which detected this candidate. The selected MA candidates can be selected by thresholding their confidence values.

V. Methodology

Our first experimental test is performed on the DiaretDB0 database [4]. This database consists of 130 uncompressed retinal images with 1500×1152 pixels resolution and 50° field-of-view (FOV). The database is split into a disjoint training and a test set. There is also manually marked MAs available for this database as ground truth. The second test is performed on the Retinopathy Online Challenge (ROC) [3], which is dedicated to the comparison of MA detectors based on their performance on 50 JPEG-compressed images different FOVs and resolution. There is also a 50 image training set available for the challenge with similar properties. For each dataset, the algorithms are compared based on the evaluation method of the ROC competition [3], which is based on the sensitivity values at seven false detections per images and on the average of these results.

VI. Results and discussion

The results for the DiaretDB0 and the ROC dataset can be seen in Tables I and II, respectively. The DRSCREEN algorithm is a former method of ours, which based on the selection of ⟨preprocessing method, candidate extractor⟩ pairs [2]. As it can be seen from the results, the proposed weighting approach provides better results on the DiaretDB0 dataset, but not on the ROC dataset. The reason for the alternating performance of the proposed and the DRSCREEN method may lie in the fact that the fundus image databases are rather different. However, both ensemble-based approach outperformed the other individual detectors which shows the strength of the ensembles in this field.

VII. Conclusion

In this paper, we presented an adaptive weighting approach for ensemble-based microanuerysm detection in color fundus images. Our approach assign weights for the candidates of the ensemble members based on their contrast and their spatial location. Our results showed that this approach is competitive with selection-based ensemble approaches and outperforms other individual detectors.

TABLE I

QUANTITATIVE RESULTS ON THE DIARETDB0 DATASET.

FP/I	1/8	1/4	1/2	1	2	4	8	avg.
DRSCREEN	0.003	0.005	0.011	0.021	0.043	0.087	0.174	0.049
proposed	**0.012**	**0.025**	**0.037**	**0.060**	**0.090**	**0.129**	**0.189**	**0.077**

TABLE II

QUANTITATIVE RESULTS OF THE ROC COMPETITION.

FP/I	1/8	1/4	1/2	1	2	4	8	avg.
DRSCREEN	0.173	0.275	0.380	0.444	0.526	0.599	0.643	0.434
proposed	**0.172**	**0.201**	**0.323**	**0.426**	**0.478**	**0.560**	**0.638**	**0.399**
Niemeijer et al.	0.243	0.297	0.336	0.397	0.454	0.498	0.542	0.395
LaTIM	0.166	0.230	0.318	0.385	0.434	0.534	0.598	0.381
ISMV	0.217	0.270	0.366	0.407	0.440	0.459	0.468	0.375
OKmedical II	0.175	0.242	0.297	0.370	0.437	0.493	0.569	0.369
OKmedical	0.198	0.265	0.315	0.356	0.394	0.466	0.501	0.357
Lazar et al.	0.169	0.248	0.274	0.367	0.385	0.499	0.542	0.355
GIB	0.190	0.216	0.254	0.300	0.364	0.411	0.519	0.322
Fujita	0.181	0.224	0.259	0.289	0.347	0.402	0.466	0.310
IRIA	0.041	0.160	0.192	0.242	0.321	0.397	0.493	0.264
Waikato	0.055	0.111	0.184	0.213	0.251	0.300	0.329	0.206

REFERENCES

[1] B. Antal and A. Hajdu, "Improving microaneurysm detection using an optimally selected subset of candidate extractors and preprocessing methods," *Pattern Recognition*, vol. 45, pp. 255–261, 2012.

[2] Bálint Antal and András Hajdu, "An ensemble-based microaneurysm detector for retinal images," in *ICIP*, 2011, pp. 1621–1624.

[3] M. Niemeijer, B. van Ginneken, M.J. Cree, A. Mizutani, G. Quellec, C.I. Sanchez, B. Zhang, R. Hornero, M. Lamard, C. Muramatsu, X. Wu, G. Cazuguel, J. You, A. Mayo, Q. Li, Y. Hatanaka, B. Cochener, C. Roux, F. Karray, M. Garcia, H. Fujita, and M.D. Abramoff, "Retinopathy online challenge: Automatic detection of microaneurysms in digital color fundus photographs," *IEEE Transactions on Medical Imaging*, vol. 29, no. 1, pp. 185–195, 2010.

[4] T. Kauppi, V. Kalesnykiene, J.-K. Kamarainen, L. Lensu, I. Sorri, H. Uusitalo, H. Klviinen, and J. Pietil, "Diaretdb0: Evaluation database and methodology for diabetic retinopathy algorithms," Tech. Rep., University of Kuopio, Finland, 2006.

[5] T. Walter and J. Klein, "Automatic detection of microaneyrysms in color fundus images of the human retina by means of the bounding box closing," *Lecture Notes in Computer Science*, vol. 2526, pp. 210–220, 2002.

[6] K. Zuiderveld, "Contrast limited adaptive histogram equalization," *Graphics gems*, vol. IV, pp. 474–485, 1994.

[7] A. A. A. Youssif, A. Z. Ghalwash, and A. S. Ghoneim, "Comparative study of contrast enhancement and illumination equalization methods for retinal vasculature segmentation," *Proc. Cairo International Biomedical Engineering Conferemce*, 2006.

[8] Rafael C. Gonzalez, Richard E. Woods, and Eddins Steven L., *Digital Image Processing Using MATLAB*, Gatesmark Publishing, 2009.

[9] A. Hoover and M. Goldbaum, "Locating the optic nerve in a retinal image using the fuzzy convergence of the blood vessels," *IEEE Transactions on Medical Imaging*, vol. 22, no. 8, pp. 951 –958, 2003.

[10] S. Ravishankar, A. Jain, and A. Mittal, "Automated feature extraction for early detection of diabetic retinopathy in fundus images," in *Computer Vision and Pattern Recognition*, 2009, pp. 210–217.

[11] A. Criminisi, P. Perez, and K. Toyama, "Object removal by exemplar-based inpainting," in *Computer Vision and Pattern Recognition*, 2003, vol. 2, pp. II–721 – II–728.

[12] Norbert Wiener, "The interpolation, extrapolation and smoothing of stationary time series," *Report of the Services 19, Research Project DIC-6037 MIT,*, 1942.

[13] T. Walter, P. Massin, A. Arginay, R. Ordonez, C. Jeulin, and J. C. Klein, "Automatic detection of microaneurysms in color fundus images," *Medical Image Analysis*, vol. 11, pp. 555–566, 2007.

[14] T. Spencer, J. A. Olson, K. C. McHardy, P. F. Sharp, and J. V. Forrester, "An image-processing strategy for the segmentation and quantification of microaneurysms in fluorescein angiograms of the ocular fundus," *Computers and Biomedical Research*, vol. 29, pp. 284–302, 1996.

[15] S. Abdelazeem, "Microaneurysm detection using vessels removal and circular hough transform," *Proceedings of the Nineteenth National Radio Science Conference*, pp. 421 – 426, 2002.

[16] T. C. Chen and K. L. Chung, "An efficient randomized algorithm for detecting circles," *Computer Vision and Image Understanding*, vol. 83, pp. 172 – 191, 2001.

[17] B. Zhang, X. Wu, J. You, Q. Li, and F. Karray, "Detection of microaneurysms using multi-scale correlation coefficients," *Pattern Recogn.*, vol. 43, no. 6, pp. 2237–2248, 2010.

[18] I. Lazar and A. Hajdu, "Microaneurysm detection in retinal images using a rotating cross-section based model," in *2011 IEEE International Symposium on Biomedical Imaging*, 2011, pp. 1405 –1409.

[19] Gyorgy Kovacs and Andras Hajdu, "Extraction of vascular system in retina images using averaged one-dependence estimators and orientation estimation in hidden markov random fields,," in *IEEE 8th International Symposium on Biomedical Imaging (ISBI2011)*, 2011, pp. 693–696.

[20] Balint Antal and Andras Hajdu, "A stochastic approach to improve macula detection in retinal images," *Acta Cybernetica*, vol. 20, pp. 5–15, 2011.

[21] L. Gagnon, M. Lalonde, M. Beaulieu, and M.-C. Boucher, "Procedure to detect anatomical structures in optical fundus images," *Medical Imaging 2001: Image Processing, Proc SPIE*, vol. 4322, pp. 1218–1225, 2001.

[22] C.J. Van Rijsbergen, *Information Retrieval*, Butterworths, London, 2nd edition, 1979.

[23] L. I. Kuncheva, *Combining Pattern Classifiers. Methods and Algorithms*, Wiley, 2004.